




## Conference Proceeding

Paper presented at the 1st International Conference on Modern Technologies in Mechanical & Material Engineering [MTME 2023]

# Tape Casting and Characterization of h-BN/PU Composite Coatings for Corrosion Resistance Applications

Atteeq Uz Zaman<sup>1</sup>, Muhammad Awais Khan<sup>1</sup>, Muhammad Waqas<sup>1</sup>, Talaal Bin Junaid<sup>1</sup>, Wardah Siddiqui<sup>1</sup>, Aqeel Ahmed<sup>2</sup>, Muhammad Ramzan Abdul Karim<sup>1\*</sup>

<sup>1</sup>Faculty of Materials and Chemical Engineering, Ghulam Ishaq Khan Institute of Engineering Sciences and Technology (GIKI), Topi- 23640, Pakistan

<sup>2</sup>Corrosion professional from the Middle East (Qatar)  
E-mail: ramzan.karim@giki.edu.pk

**Received:** 25 May 2023; **Revised:** 3 August 2023; **Accepted:** 7 August 2023

**Abstract:** In the present work, a slurry of polyurethane (PU) was prepared by adding various contents (3 and 8 wt.%) of hexagonal boron nitride (h-BN). Ethanol was utilized as a solvent to reduce the viscosity and sticking effect of the PU. The mixture was then applied as polymer matrix composite (PMC) coating on steel substrates via tape casting. The prepared coatings were characterized for their structure, adhesion and thermal properties, and corrosion resistance characteristics. The structural and morphological features of the h-BN/PU composites were characterized by X-ray diffraction (XRD) and scanning electron microscopy (SEM). Rockwell-C adhesion tests were conducted to examine the adhesion between the substrate and composite coating. The potentiodynamic polarization tests were utilized to assess the anti-corrosion performance of composite coatings when applied and steel substrates. The results exhibited that the inclusion of h-BN filler (3 wt.%) could effectively enhance the anti-corrosion performance of the h-BN/PU composite. The reason for the improvement in corrosion properties was attributed to lower surface roughness, uniform distribution and great adhesion strength of PU/3 wt.% h-BN composite. Furthermore, the PU/3 wt.% h-BN composites showed relatively improved thermal stability and higher glass transition temperature (T<sub>g</sub>). However, further loading of h-BN contents (8 wt.%) deteriorates the thermal and corrosion resistance properties of the composite due to the clustering of h-BN, which creates localized areas of increased corrosive activity.

**Keywords:** PMC, PU, h-BN, corrosion resistance, thermal degradation

## 1. Introduction

Metallic materials often experience a reduction in durability due to their corrosion process. Corrosion is the natural degradation of metallic materials caused by chemical interactions with reactive substances in their surroundings such as salt, oxygen, and water [1]. As a consequence, the chemical stability and mechanical properties of the metal deteriorate, resulting in both economic losses and adverse environmental effects. During ancient times, beeswax and animal fat were employed on metal surfaces to inhibit the corrosion process. Nowadays, significant progress has been in the development of advanced protective technologies with remarkable anti-corrosion characteristics along with low

permeability.

Among this advancement, solvent-based anticorrosive coatings have gained significant attention owing to their low cost, chemical stability, and amazing ability to build a strong physical barrier against corrosive electrolytes such as salts, oxygen and water. Among all solvent-based anticorrosive coatings, polyurethane (PU) stands out owing to its low weight, high flexibility, exceptional chemical resistance, outstanding weather ability, and excellent adhesion to substrates [2]. However, the poor wear and corrosion resistance of PU has posed limitations on its application in harsh environments.

To address these challenges, several reinforcements such as clay [3], carbon nanotubes [4], SiO<sub>2</sub> [5], TiO<sub>2</sub> [6], Al<sub>2</sub>O<sub>3</sub> [7] and hexagonal boron nitride (h-BN) [8] have been incorporated into PU composites to improve its tribological, corrosion resistance and thermal properties. Among these, h-BN exhibits outstanding thermal and chemical stability, excellent electrical insulation, biocompatibility, chemical inertness, and good water resistance [9]. In this study, a tape casting technique was used to prepare PU composite coating by the inclusion of varying concentrations of h-BN (0 wt.%, 3 wt.% and 8 wt.%). The main objective of this work is to assess the morphological, thermal and chemical (corrosion) resistance properties of h-BN/PU composite coating.

## 2. Materials and methods

### 2.1 Materials

PU in resin form was obtained from Shandong, China. h-BN powder provided was also imported from China (average particle size of 1 μm, 99% purity) and was utilized as a reinforcement material. Ethanol was used in the experiment as a solvent to reduce the viscosity of PU.

### 2.2 h-BN/PU composite preparation

The raw materials PU and h-BN powder were vigorously hand mixed for 5 minutes in ethanol to prepare a homogeneous slurry. Ethanol was added to reduce the viscosity of the slurry and prevent it from sticking to the mild steel substrate during the tape-casting process. Before mixing, h-BN powder underwent grinding in a mortar and pestle to decrease particle size and prevent clumping. The slurry was placed in a vacuum desiccator at 550-600 mm Hg to remove entrapped air. Using a doctor blade coating machine, set up to a 1 mm gap of micrometers, the slurry was spread onto mild steel substrate by the doctor blade moving at a horizontal speed of 250 mm/minute. The tape was then air-dried to produce continuous crack-free tapes on the substrate for further characterization. The schematic for the experimental steps is shown in Figure 1.

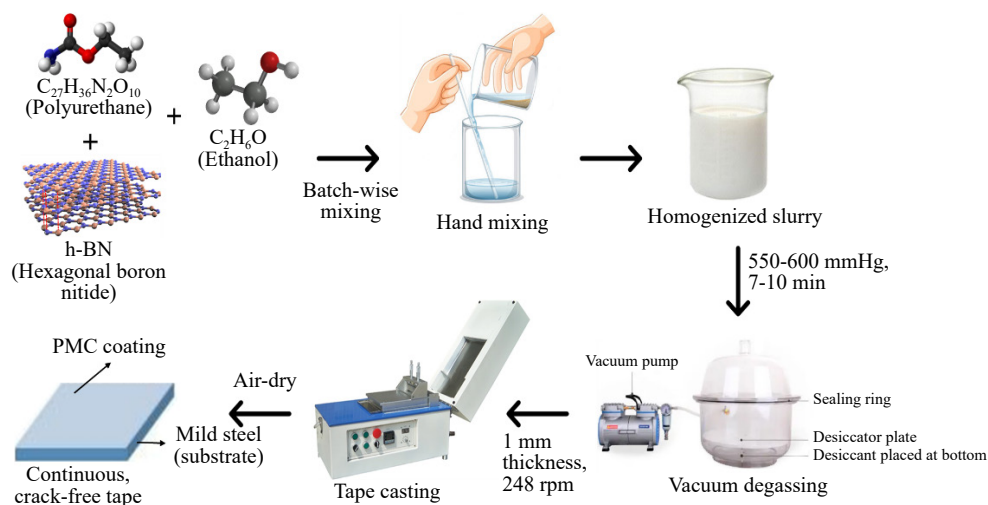


Figure 1. Experimental steps flow diagram for slurry making and subsequent tape casting

## 2.3 Characterization tools

The morphology and compositional analysis of the fabricated h-BN/PU composite were investigated using scanning electron microscopy (SEM) (Carl Zeiss Evo 15). X-ray diffraction (XRD) analysis (Proto Manufacturing Ltd, Canada) was performed to determine the crystal structure, phases and planes of fabricated composites, scanning with the scan rate of 2°/min, between the angle range of  $20^\circ \leq 2\theta \leq 80^\circ$ . Adhesion properties of the h-BN/PU coatings were evaluated through the Rockwell-C adhesion test with a diamond cone indenter, applying a load of 600 N for a dwell time of 15 seconds. The resulting indentation imprints were compared with standard images provided in the test standard to determine the level of adhesion. The adhesion scale utilized for visual inspection is illustrated in Figure 2 [10]. The test defines different levels of adhesion, with HF1-HF4 representing adequate adhesion (indicating acceptable coating quality), while HF5 and HF6 indicate insufficient adhesion. For differential scanning calorimetry (DSC) and thermogravimetric analysis (TGA), a Simultaneous Thermal Analyzer (STA-8000) from Perkin Elmer, USA was utilized. The analysis was conducted at a 30 °C to 800 °C temperature range with a heating rate of 10 °C/min in a nitrogen environment to minimize the effects of oxidation.

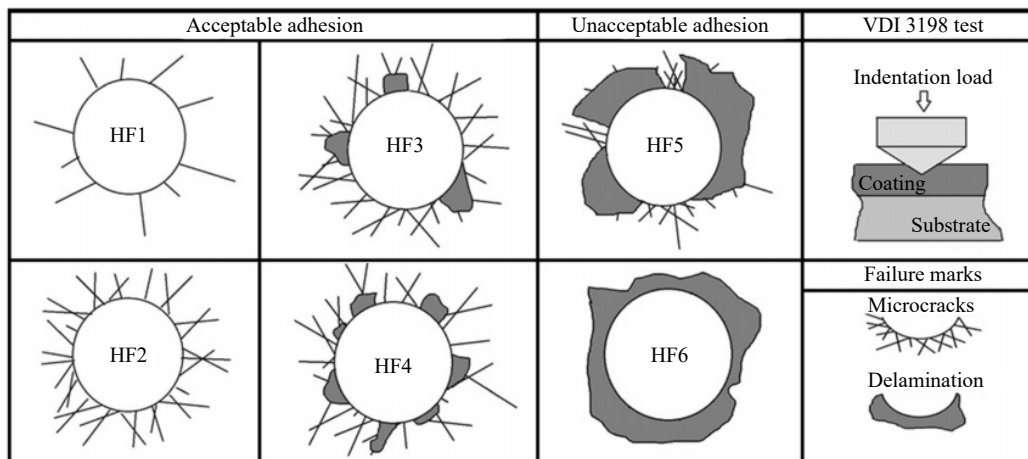


Figure 2. The VDI3198 scale for comparing indented specimens to evaluate adhesion characteristics [10]

## 2.4 Corrosion properties testing

The corrosion properties of the PU composite coatings were evaluated by utilizing the potentiodynamic polarization technique. The measurements were done by a Reference 3000 potentiostat/galvanostat system by Gamry, USA, in a three electrodes electrochemical cell. The substrates coated with the prepared h-BN/PU composites having an exposed surface area of 4 cm<sup>2</sup> acted as working electrodes whereas, Ag/AgCl and Pt wire acted as the reference electrode and counter electrode respectively. The corrosion resistance was calculated via the Echem Analyst software by using the Tafel fitting method.

## 3. Results and discussion

### 3.1 Surface morphology via SEM analysis

The surface morphology of the tapes with different compositions was analyzed using the SEM characterization technique. As evident in Figures 3(a) and 3(b), it was noticed that the h-BN particles in the matrix were homogeneously dispersed without any voids or cracks at the surface in case of low concentration of h-BN (3 wt.%). However, further loading of h-BN up to 8 wt.% exhibited agglomeration of h-BN particles as shown in Figures 3(c) and 3(d). This agglomeration increases the surface roughness and ultimately decreases the corrosion resistance. Therefore,

the composite incorporated with 8 wt.% h-BN disclosed lower corrosion resistance as evidenced by the corrosion rate results presented in the corrosion studies section at the end. On the other hand, it can be said that lower surface roughness will result in a decreased corrosion rate [11], and hence the PU coating with 3 wt.% h-BN depicts a low corrosion rate and higher resistance.

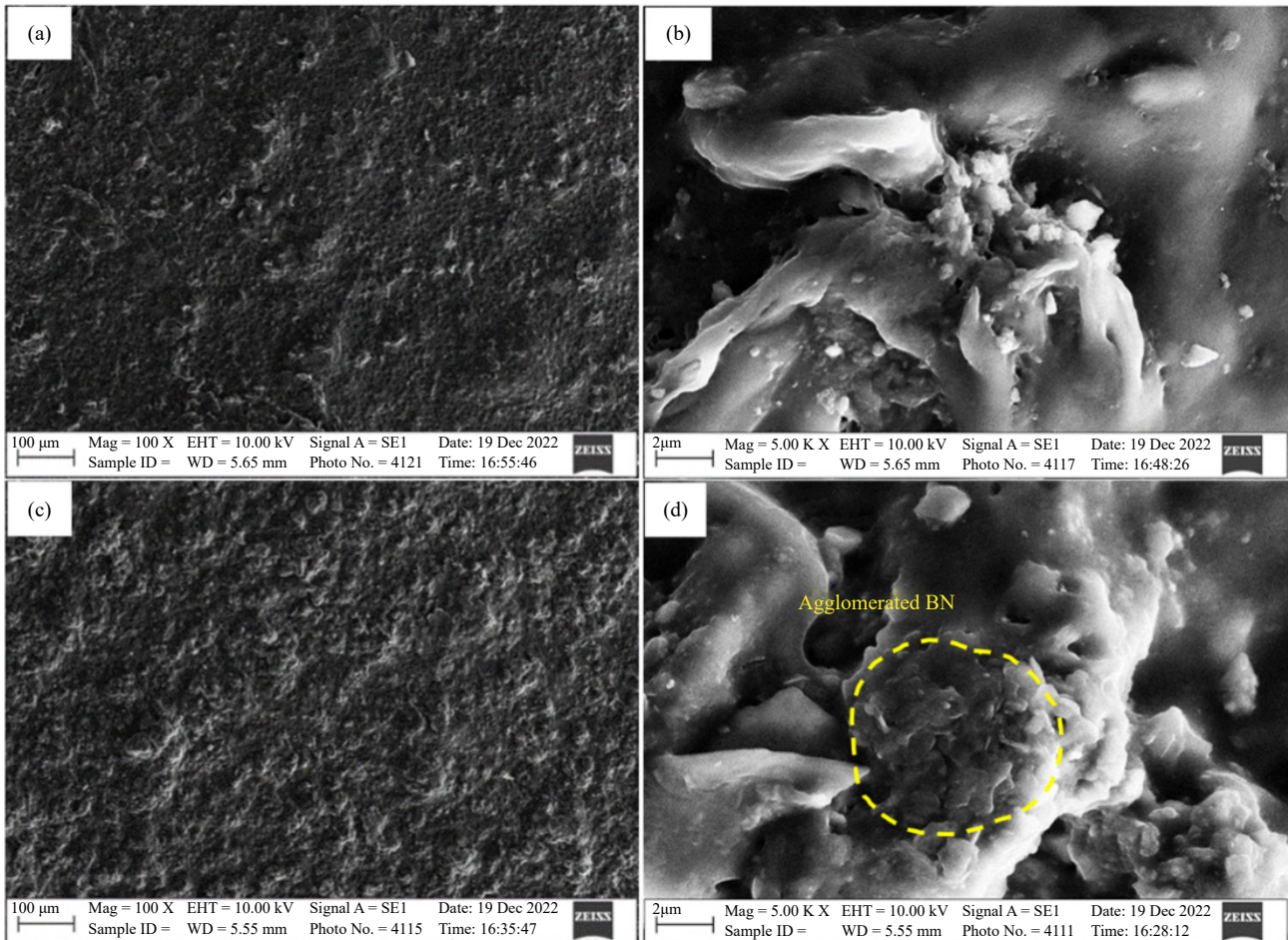


**Figure 3.** SEM micrographs of h-BN/PU composites: (a) and (b) PU/3 wt.% h-BN, (c) and (d) PU/8 wt.% h-BN

### 3.2 XRD analysis

The XRD spectra of PU/3 wt.% h-BN and PU/8 wt.% h-BN composites are presented in Figure 4. The analysis of the spectra revealed that the characteristic peaks appeared at  $28^\circ$ ,  $42^\circ$ ,  $44^\circ$ ,  $50^\circ$ ,  $55^\circ$  and  $76^\circ$  endorse the presence of BN. Furthermore, peaks found at  $21.3^\circ$  and  $25.5^\circ$  confirmed the existence of PU. Notably, no reaction peaks were observed, demonstrating that PU and h-BN did not undergo any chemical reaction to form a new phase. This result confirmed the preservation of the individual characteristics of PU and h-BN within the polymer matrix composite (PMC), indicating minimal alteration to the crystal structure of PU by the addition of h-BN.

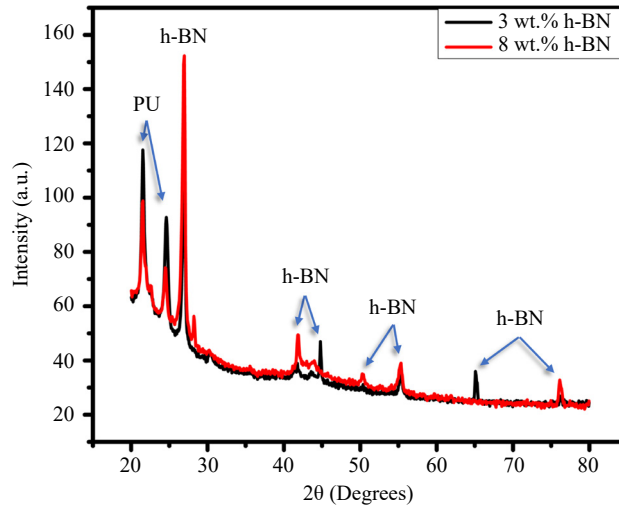


Figure 4. XRD spectra for prepared h-BN/PU composites

### 3.3 Adhesion evaluation via Rockwell hardness (HRC) tests

Figure 5 depicts the optical micrographs of the indentation craters of the composites containing 3 wt.% and 8 wt.% h-BN after the Rockwell-C adhesion test [12]. Damage to the h-BN/PU coating and adhesion strength was defined according to the VDI3198 scale that has been presented in Figure 2. In Figure 5(a), it can be observed that the delamination of the coating from the mild steel substrate in the crater region was identified in the PU/8 wt.% h-BN composite. This delamination or scaling defect was due to the weak adhesion between the substrate and h-BN/PU coating. Therefore, the images of the samples according to the quality test were identified as HF6 and represent inadequate adhesion. However, strong adhesion of the coating to the mild steel substrate was observed in PU/3 wt.% h-BN composite and was among the acceptable failures (HF1) according to the VDI3198 scale (see Figure 5(b)).

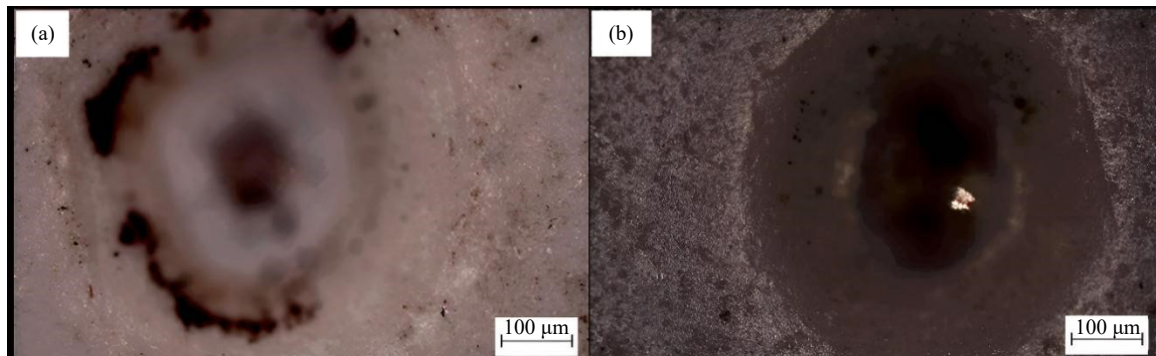


Figure 5. Micrographs after indentation for adhesion evaluation of (a) PU/8 wt.% h-BN; (b) PU/3 wt.% h-BN

### 3.4 Thermal analysis (DSC/ TGA)

DSC-TGA curves were obtained to identify the presence and the influence of reinforcement content on crystallization behavior, melting point and thermal stability of the h-BN/PU composite materials under varying temperature conditions. Figure 6(a) demonstrated the comparison of DSC curves of 3 wt.% and 8 wt.% h-BN composite, revealing a slight increase in the glass transition temperature ( $T_g$ ) with higher h-BN additions. In polymers, the glass transition is a complex mechanism that depends on several aspects. In this work, it was expected that the interaction between h-BN and the matrix and free volume will have a significant impact on the  $T_g$  of PU. The coupling of PU

groups on the surface of h-BN particles can interact with the curing substance or become interconnected with the PU chains. This strengthened the inter-facial contacts between the matrix and fillers, effectively reducing the free space for the epoxy chains. Thermal analysis using DSC demonstrated that incorporating 3 wt.% h-BN into PU led to significant enhancements in conversion and Tg of the composite matrix. However, increasing the h-BN content leads to a decline in Tg due to the presence of air voids and insufficient bonding at the interfaces [13].

Furthermore, it was evident from Figure 6(b) that the inclusion of h-BN filler has minimal impact on the onset temperature of thermal degradation of h-BN/PU composites. The curves indicated the PU polymer chains were primarily responsible for the degradation of the composite below 450 °C. However, the addition of h-BN significantly inhibits the degradation of composites at elevated temperatures, such as 450 °C and 600 °C, due to their substantial shielding effect. Consequently, the breakdown products are delayed from exiting the PU polymer. Moreover, the TGA analysis demonstrated that these composites exhibited remarkable resistance to extremely high temperatures during service, preventing extensive combustion or thermal degeneration. It is noteworthy that the inclusion of h-BN has no impact on the thermal performance of PU composite at elevated temperatures [14]. The numerical thermal characteristics values of the h-BN/PU composites are tabulated in Table 1.

**Table 1.** Thermal characteristics values of h-BN/PU composites

Composition	Melting temperature (Tm)	Glass transition temperature (Tg)	Composition	Thermal degradation temperature
PU with 3 wt.% h-BN	400 °C	50 °C	PU with 3 wt.% h-BN	380 °C
PU with 8 wt.% h-BN	380 °C	52 °C	PU with 8 wt.% h-BN	300 °C

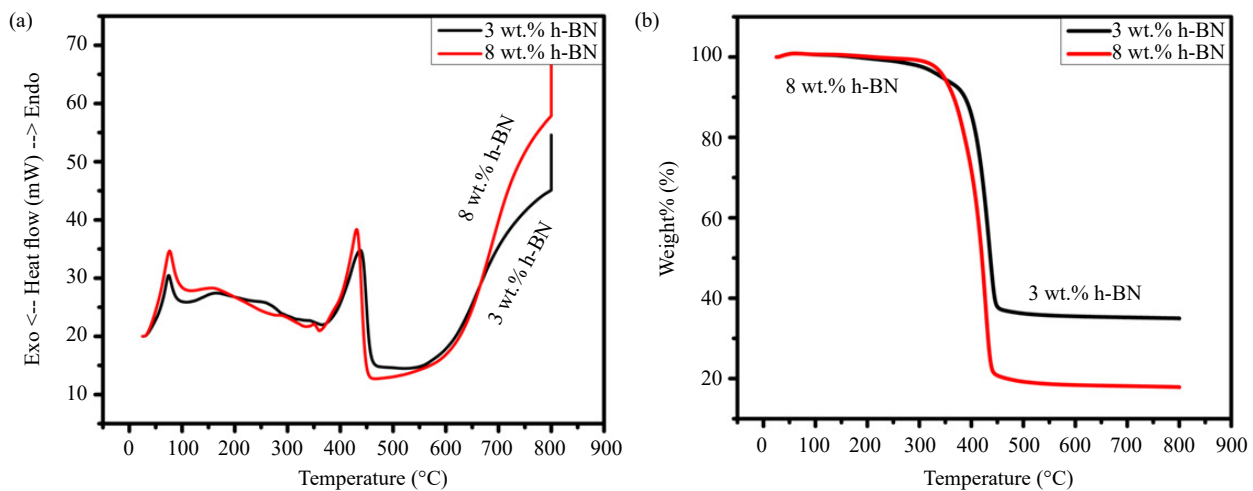


**Figure 6.** Thermal analysis of h-BN/PU composites: (a) DSC curves, (b) TGA curves

### 3.5 Corrosion properties analysis

The corrosion tests were performed on uncoated and coated (with PU/3 wt.% h-BN, PU/8 wt.% h-BN) mild steel substrates for comparative analysis. The potentiodynamic polarization curves obtained from the corrosion tests are presented in Figure 7, while comprehensive electrochemical numerical data obtained from Tafel fitting is given in Table 2. Analysis of the graphs in Figure 7 revealed that the sample coated with PU/3 wt.% h-BN exhibited a lower current density and a higher potential value, indicating a higher corrosion resistance compared to the other samples. This enhanced corrosion resistance can be ascribed to the even dispersion of h-BN particles within the PU matrix, which acts as an effective barrier against corrosion. However, for PU/8 wt.% h-BN composite, the higher concentration of h-BN particles resulted in the formation of agglomerates or clusters, creating localized areas of increased corrosive

activity. Consequently, the overall resistance of the composite to corrosion was lowered. Figure 7 also illustrates that the uncoated sample displayed a corrosion rate of 17.95 mpy, while the coated composite (3 wt.% h-BN) exhibited a significantly reduced corrosion rate of 0.006 mpy. This substantial reduction in corrosion rate demonstrated the excellent corrosion resistance provided by the PU/3 wt.% h-BN coated sample.

**Table 2.** Parameters obtained from Tafel fitting of potentiodynamic polarization curves

Composition	Beta(A) (volt/decade)	Beta(C) (volt/decade)	$I_{corr}$ (ampere)	$E_{corr}$ (mV)	Corrosion rate (mpy)
0 wt.% h-BN	92.88-3	511.8-3	155.2-6	-547.2	17.95
3 wt.% h-BN	1.21	1.123	55.6-9	-136	0.006
8 wt.% h-BN	331.6-3	406.2-3	21.70-6	-625.5	2.518

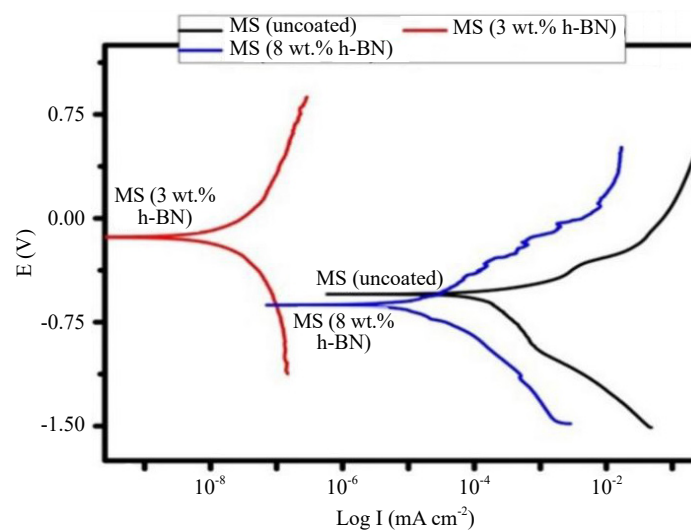


**Figure 7.** Potentiodynamic polarization curves obtained from electrochemical corrosion tests performed on uncoated mild steel substrates and the substrates coated with h-BN/PU composites

## 4. Conclusions

PU-based PMC coatings were successfully fabricated by the inclusion of various concentrations (0 wt.%, 3 wt.% and 8wt.%) of h-BN. The purpose was to assess the impact of h-BN on the micro-structure, crystal structure, thermal behavior and corrosion protection potential of the composites. The micro-structural analysis demonstrated uniform dispersion of h-BN (when in low concentration) within PU PMC, contributing to the enhanced corrosion resistance, by acting as an effective barrier against corrosion. However, the increased concentration of h-BN led to the formation of agglomerates or clusters, creating localized areas of increased surface roughness ultimately leading to enhanced corrosive activity. TGA and DSC analysis showed that the composites have got improved thermal stability and a higher Tg in the case of a low concentration of h-BN. The adhesion test via HRC hardness tests showed that the 3 wt.% h-BN polymer composite coating has excellent adhesion properties. In conclusion, the findings indicate that the developed h-BN composite coatings (3 wt.%) have promising potential for their use in applications requiring corrosion resistance.

## Acknowledgments

The authors acknowledge the Higher Education Commission (HEC) of Pakistan for providing financial assistance

via its National Research Program for Pakistani Universities (Project No. HEC-NRPU # 10493). We also acknowledge the constructive feedback of Dr Hamza Mohsin, Dr Tauheed Shehbaz and Mr Waseem Shehzad (PhD Scholar) from the Faculty of Materials and Chemical Engineering.

## Conflict of interest

There is no conflict of interest for this study.

## References

- [1] Frankel GS. Pitting corrosion of metals: a review of the critical factors. *Journal of the Electrochemical Society*. 1998; 145(6): 2186. <https://doi.org/10.1149/1.1838615>
- [2] Chattopadhyay DK, Prasad PSR, Sreedhar B, Raju KVS. The phase mixing of moisture cured polyurethane-urea during cure. *Progress in Organic Coatings*. 2005; 54(4): 296-304. <https://doi.org/10.1016/J.PORGCOAT.2005.07.004>
- [3] Abd El-Fattah M, El Saeed AM, Dardir MM, El-Sockary MA. Studying the effect of organo-modified nanoclay loading on the thermal stability, flame retardant, anti-corrosive and mechanical properties of polyurethane nanocomposite for surface coating. *Progress in Organic Coatings*. 2015; 89: 212-219. <https://doi.org/10.1016/J.PORGCOAT.2015.09.010>
- [4] Wang T, Yu WC, Zhou CG, Sun WJ, Zhang YP, Jia LC, et al. Self-healing and flexible carbon nanotube/polyurethane composite for efficient electromagnetic interference shielding. *Composites Part B: Engineering*. 2020; 193: 108015. <https://doi.org/10.1016/J.COMPOSITESB.2020.108015>
- [5] Maganty S, Roma MP, Meschter SJ, Starkey D, Gomez M, Edwards DG, et al. Enhanced mechanical properties of polyurethane composite coatings through nanosilica addition. *Progress in Organic Coatings*. 2016; 90: 243-251. <https://doi.org/10.1016/j.porgcoat.2015.10.016>
- [6] Taheran M, Navarchian AH, Razavi RS. Optimization of wear resistance of PU/TiO<sub>2</sub> coatings on aluminum surfaces. *Progress in Organic Coatings*. 2011; 72(3): 486-491. <https://doi.org/10.1016/J.PORGCOAT.2011.06.007>
- [7] Chen CH, Wang JJ, Yen FS. Preparation and tribological properties of polyurethane/ $\alpha$ -aluminum oxide hybrid films. *Thin Solid Films*. 2010; 518(24): 7515-7518. <https://doi.org/10.1016/J.TSF.2010.05.036>
- [8] Yang X, Zhang R, Pu J, He Z, Xiong L. 2D graphene and h-BN layers application in protective coatings. *Corrosion Reviews*. 2021; 39(2): 93-107. <https://doi.org/10.1515/correv-2020-0080>
- [9] Abdul Karim MR, Khan MA, Zaman AU, Hussain A. Hexagonal boron nitride-based composites: An overview of processing approaches and mechanical properties. *Journal of the Korean Ceramic Society*. 2023; 60(1): 1-23. <https://doi.org/10.1007/s43207-022-00251-8>
- [10] Kayali Y, Taktak S. Characterization and Rockwell-C adhesion properties of chromium-based borided steels. *Journal of Adhesion Science and Technology*. 2015; 29(19): 2065-2075. <https://doi.org/10.1080/01694243.2015.1052617>
- [11] Kear G, Barker BD, Stokes K, Walsh FC. Flow influenced electrochemical corrosion of nickel aluminium bronze—Part I. Cathodic polarisation. *Journal of Applied Electrochemistry*. 2004; 34: 1235-1240. <https://doi.org/10.1007/S10800-004-1758-1>
- [12] Broitman E, Hultman L. Adhesion improvement of carbon-based coatings through a high ionization deposition technique. *Journal of Physics: Conference Series*. 2012; 370(1): 012009. <https://doi.org/10.1088/1742-6596/370/1/012009>
- [13] Çakmakçı E, Koçyiğit Ç, Çakır S, Durmus A, Kahraman MV. Preparation and characterization of thermally conductive thermoplastic polyurethane/h-BN nanocomposites. *Polymer Composites*. 2014; 35(3): 530-538. <https://doi.org/10.1002/pc.22692>
- [14] Gul S, Arican S, Cansever M, Beylergil B, Yildiz M, Saner Okan B. Design of highly thermally conductive hexagonal boron nitride-reinforced PEEK composites with tailored heat conduction through-plane and rheological behaviors by a scalable extrusion. *ACS Applied Polymer Materials*. 2022; 5(1): 329-341. <https://doi.org/10.1021/ACSAPM.2C01534>